Continued Development of Broadband Passive Bearing Estimation

Steven J McManus
Teledyne Benthos, Inc.
49 Edgerton Drive
North Falmouth, MA 02556 USA
sjmcmanus@teledyne.com

Dale Green
Teledyne Benthos, Inc.
49 Edgerton Drive
North Falmouth, MA 02556 USA
dale.green@teledyne.com

Abstract-- **One of the major challenges in open-ocean deployment of unmanned underwater vehicles (UUVs) or unmanned surface vehicles (USVs) is collision avoidance with approaching surface shipping. Existing methods assume that the underwater robot carries a radar and/or has access via radio to commercial Automatic Identification System (AIS) information. However, radars are expensive and both radars and radio can only operate above the water. Moreover, AIS status is not always broadcast by passing shipping.**

An alternative solution may be found through the use of underwater acoustics whereby a sonar system determines the direction of arrival for a surface ship based upon the ship's radiated noise. The effectiveness of this method lies in the use of as much of the radiated frequency spectrum as is practically accessible, hence a broadband sonar is preferred. We refer to our device as the Passive Bearing Detector (PBD).

Ultra-short baseline (USBL) is a well-known interferometric method for estimating the direction of arrival for *known narrowband* acoustic signals. In this paper, we discuss a method that supports direction of arrival estimation for *any wideband* source of acoustic energy without *a priori* knowledge of the specific temporal or spectral characteristics of the signal. In support of this, we build an array of several listening hydrophones that are spaced at a pre-determined distance in a known geometry. The spacing among hydrophones is dictated by the upper limits of the frequency band, while the available bandwidth then is limited by the mismatch between array aperture and source wavelength. Our broadband interferometric algorithm provides estimates of azimuthal arrival angle, but the accuracy of the algorithm for such a small and compact array is highly dependent on variable channel conditions. We compare the performance of conventional and adaptive beamforming techniques applied to PBD data recorded at sea. We demonstrate that our approach is far less computationally intensive, but appears to perform as well as or better than the beamformers.

An extensive sea trial was conducted at an acoustic test range in Northern Europe. We review performance of our system and further demonstrate the qualities of a bearings-only tracker and the (future) ability to autonomously extract snippets of time series, conduct time-series analyses, compress the results, and provide the result for telemetry via our integrated acoustic communications.

Keywords--Acoustic communications, modems, passive sonar, bearing estimation, USBL

1. INTRODUCTION

This paper represents a continuation of our efforts to develop long term, autonomous monitoring of ocean sources of noise. Applications include marine preserves, collision avoidance, and perhaps piracy.

In the underwater environment, most man-made sources of acoustic energy are highly directional in azimuth, and often in the vertical plane as well. Passive sonars, utilizing discrete-element beamformers or crudely-directional transducers (e.g., DIFAR) have been used for decades for estimating the directions of arrival (DOAs) for both narrow band and broad band sources of acoustic energy. These approaches are often: physically large; costly, computationally expensive; and not especially accurate. Our interest is in developing low cost, physically small, battery-powered devices for the same purposes.

Unmanned platforms on or near the sea surface are at danger of collision with other shipping, especially if the platform lacks radar and/or the other vessel is not radiating its Automatic Identification System (AIS) status. Fortunately, most surface vessels utilize some form of propulsion system which generates broadband acoustic energy. We can make use of this energy to estimate the direction of arrival (DOA) if we have a system properly tuned for the frequency band of the energy.

An earlier paper [1] provided an overview of the PBD and described performance in several sea trials. The impetus for this paper was a recent sea trial conducted at an acoustic tracking range. This 4-day demonstration provided environments with high sea state noise, nearby shipping, and manoeuvring targets. PBD DOA estimates were made in real time by the autonomous sensor. Post-trials processing of recorded data was employed to refine our bearings-only tracker, to apply a variety of beamformers to the recorded time series, and to develop single-hydrophone time series extraction and manipulation for target signature analyses. In

978-0-933957-43-5 ©2015 MTS

future, some or all of these capabilities will be integrated into the real-time autonomous sensor system.

In its present configuration, the PBD makes a DOA estimate every 4 seconds. There will always be an estimate, provided a certain quality threshold is passed, but the existing, basic system uses no *a priori* knowledge of past measurements. Each estimate is completely independent of all others, and may reflect a source of interest, multiple sources, or random sea noise. Figure 1 shows a brief time history of PBD measurements, most of which fit the random category, but others apparently forming temporal tracks – provided a human eye is available to make such a judgement.

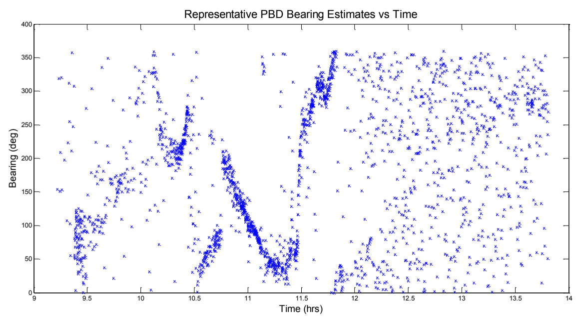

Fig. 1. A representative example of PBD bearing estimates vs. time.

Section 2 describes the several DOA estimation techniques that have been investigated. Section 3 discusses recent experimental results in DOA estimation and tracking, while section 4 considers time series analyses. Section 5 provides conclusions

2. BEARING ESTIMATION

We assume an array of K small hydrophones each sensing the signal and ambient noise. Let R_X and R_N be the autocorrelation functions of signal x(t) and noise n(t), respectively. The noise is assumed to be independent of the signal, but without appreciable loss in generality we assume that the noise bandwidth is the same as the signal bandwidth W. The arbitrary signal duration is denoted by T, but the product TW >> 1. This signal arrives at all hydrophones from an angle Θ relative to a reference angle, as described in Figure 2 (note that K=2 is the minimally acceptable number of hydrophones). The element locations are described by the matrix $\mathbf{P} = [\underline{p}1, \ldots \underline{p}4]$, with $\underline{p}_k = \{x_k, y_k, z_k\}^T$. The element at the upper vertex is arbitrarily considered as the first element.

A. PBD DOA Estimates

We compute the sample auto and cross correlations of the signal plus noise between the reference hydrophone and each of the others. We sample the phase of the correlations at the same instant in time. For our tetrahedral geometry case, we form a vector of phase differences $\underline{\boldsymbol{\delta}}$, which we treat as a time-difference vector. The phase angle between complex correlations is obtained from

$$\underline{\mathbf{v}} = \mathbf{P}\boldsymbol{\delta}. \qquad (1)$$

The desired PBD azimuthal bearing to the target is obtained as

$$\Theta = \mathrm{atan}(\underline{\mathbf{v}}(1), \underline{\mathbf{v}}(2)) \qquad (2)$$

while the vertical angle is obtained as

$$\Phi = \mathrm{atan}(\underline{\mathbf{v}}(3)/||\underline{\mathbf{v}}||) \qquad (3)$$

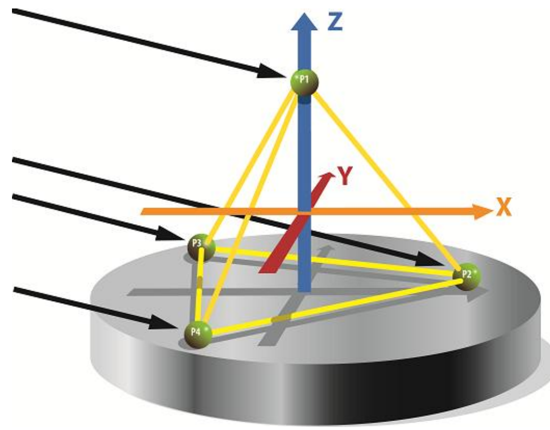

Fig. 2. A regular tetrahedral geometry suitable for PBD direction of arrival angle estimation.

We "tune" the PBD by separating the hydrophones to accommodate the frequency band of interest. For example, for a frequency band of 9 – 14 kHz, hydrophone spacing in a tetrahedral shape is approximately 5 cm, while a frequency band of 1600 Hz to 3600 Hz can be accommodated with a hydrophone spacing of approximately 20 cm. There is always a lower frequency edge to the band below which artifacts will appear in the DOA estimation. The algorithm is well served by a good quality bandpass filter to isolate the band of interest from broader signature components, as well as to isolate the unit from out-of-band interference.

Similar to many simple interferometric systems, the PBD is only suitable for processing a single source of energy at one time. If two or more energy sources are received at the same time, the PBD will respond with a DOA estimate somewhere between the sources – depending on the relative signal strength.

B. Conventional Beamforming (CBF)

The T-seconds of data received on the k^{th} array element is assumed to be an unknown, bandlimited but wideband signal. We assume it to be properly basebanded[1] as an analytic time

[1] By baseband we refer to the modification of a passband signal into a single-sideband signal heterodyned such that the carrier

series $x_k(n)$, where n is a time index. Data are bandlimited to W Hz, with a duration of Z samples for each element and are collected in a matrix **X** of K columns and N rows. We are able to form a "conventional" beam [2, Chapter 1] in the horizontal and vertical directions $\{\boldsymbol{\theta}_m\ \Phi_m\}$ by developing a steering vector of weights $\underline{\mathbf{s}}_k$ with the k^{th} element with respect to the m^{th} source defined as

$$s_{km} \approx \exp(-i2\pi F_0 d_{km} / c) \tag{4}$$

In eqn (4) F_0 is the center frequency of the band, c is the sonic speed. If R_m is the Cartesian coordinate of a <u>hypothesized</u> distant source in the direction $\{\boldsymbol{\theta}_m\ \Phi_m\}$, then

$$d_{km} = \| ((\underline{R}_m - \underline{p}_k) \| \tag{5}$$

where the symbol $\|\ \|$ indicates Euclidean norm. In the case of applying this weight to the broadband signal, the beam power in the desired direction is obtained simply as

$$J_m = \| \underline{\mathbf{s}}^H_m \mathbf{X} \|^2 \tag{6}$$

where $()^H$ indicates Hermetian transpose. An alternative and useful version of the CBF beam power is

$$J_m = \underline{\mathbf{s}}^T_m \mathbf{Q} \underline{\mathbf{s}}_m \tag{7}$$

where **Q** is the sample covariance matrix

$$\mathbf{Q} = \mathbf{X}\mathbf{X}^H \tag{8}$$

We note that eqn (8) is only valid for narrow band data, or approximately for cases in which $W << F_0$. Nevertheless, as we will show it is a useful tool for our application.. We also note that equations (4) through (8) are pertinent to a single "look" direction. However, there is no *a priori* knowledge that a source is present at that location. Our solution is to conduct an (approximate) maximum likehood search by incrementing both (hypothesized) $\boldsymbol{\theta}_m$ and Φ_m by a small amount around the region of interest – perhaps a complete sphere if no other information is present. This computational burden is significant, and can be greatly reduced when performed in conjunction with the phase-based PBD algorithm,

C. MVDR Beamforming

We can extend the CBF approach to an MVDR approach by replacing the steering vector $\underline{s}_m$ by a weight vector $\underline{w}_m$, obtained as follows.

Let $\mathbf{Q}^{-1}$ be the inverse of the covariance matrix **Q**. We obtain this via a singular value decomposition (SVD) of covariance matrix **Q** that provides us with associated eigenvectors and eigenvalues.. By substituting

$$\underline{\mathbf{w}}_m = \mathbf{Q}^{-1}\underline{\mathbf{s}}_m \,/\, (\underline{\mathbf{s}}^H_m \mathbf{Q}^{-1}\underline{\mathbf{s}}_m) \tag{9}$$

for $\underline{\mathbf{s}}_m$ in eqn (7) we obtain MVDR beam power in the direction $\{\theta_m\ \Phi_m\}$.

D. Subband Beamforming of Broadband Signals

Equation (6), using either CBF or MVDR weights is suboptimal if bandwidth W is too large relative to the center frequency [2, Chapter 2]. We can overcome this problem by first dividing the data on each array element into narrow subbands, using analysis filters [2, Chapter 3]. We choose to do this using non-overlapping short term FFTs to compute a (complex) spectrogram. The temporal output of each FFT bin is used for independent beamforming, then all subbands are recombined via an IFFT to obtain total "beam" power..

2.1.1 <u>Subband MVDR</u>

In eqn (4) we replace F_0 with the exact frequency represented by the j^{th} FFT bin, which we call Fj. In eqn (6) we replace the data matrix **X** with a matrix $\mathbf{Y}_j$ containing all of the temporal samples from the j^{th} FFT bin. We replace **Q** in eqn (7) with $\mathbf{Q}_j$, and $\mathbf{Q}^{-1}$ in eqn (9) with $\mathbf{Q}^{-1}_j$. We find conventional weights $\underline{\mathbf{s}}_{mj}$ according to eqn (4), and MVDR weights $\underline{\mathbf{w}}_{mj}$ according to eqn (9). However, in place of eqn (7) we obtain beam power by using

$$J_m = |\textstyle\sum_{j=1}^{J} \mathrm{ifft}(A^H{}_{mj} \boldsymbol{Y}_j)|^2 \tag{10}$$

where $\underline{A}_{mj}$ is either the CBF or MVDR steering vector for the j^{th} FFT bin.

2.1.2 <u>Subband, Modified MVDR (MMVDR)</u>

When computing the inverse covariance matrix, the (ordered) eigenvectors $\underline{\boldsymbol{\mu}}$ and associated eigenvalues $\underline{\boldsymbol{\lambda}}$ may be obtained, say, via a singular value decomposition. We make an assumption that for distinct sources the individual eigenvectors associated with strong eigenvalues are each associated with a unique source. Given that we only want to estimate the bearing for a single target, we modify the MVDR weight vector with the eigenvector $\underline{\boldsymbol{\mu}_1}$ corresponding to the largest eigenvalue $\boldsymbol{\lambda}_1$ as follows:

$$\underline{\hat{\boldsymbol{w}}}_{mj} = (\boldsymbol{\mu}_1 \boldsymbol{\mu}_1^H)\underline{\mathbf{w}}_{mj} \tag{11}$$

We then substitute $\underline{\hat{\boldsymbol{w}}}_{mj}$ for A_{mj} in eqn (10) and calculate the MMVDR beam power for this (presumed) single source. We note that eqn (11) is similar to, but significantly different from the MUSIC algorithm [3], which projects the <u>noise</u> subspace onto the steering vectors. MUSIC is used for obtaining DOA, but does not provide a time series for further processing.

E. Example Bearing Estimation Results

In Figures 3 and 4 we show one example each for the various beamformers. On both figures we show the PBD bearing estimate (196.3 deg) and the estimate obtained from

frequency resides at 0 Hz, and with a sample rate appropriate for the bandwidth.

the peak of the beamformer curve. The resolution of each beamformer is 2 degrees. We observe that CBF broadband (and narrowband – not shown) provide comparable bearings, but show little to no gain. The other approaches provide comparable bearing estimates, but offer considerable spatial directivity.

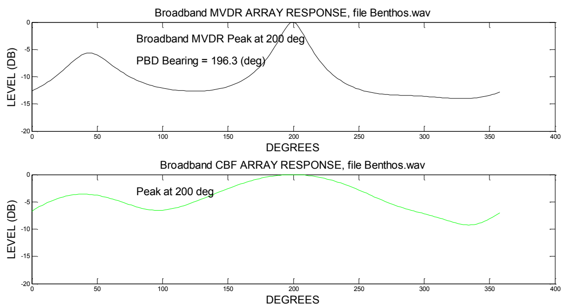

Fig. 3. Broadband CBF and MVDR

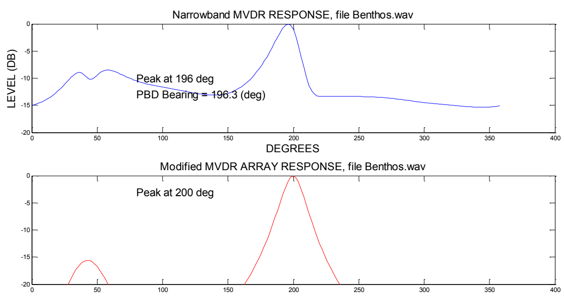

Fig. 4. Subband MVDR and subband MMVDR

The PDB computation is a single matrix-matrix multiply, folowing by two inverse tangent equations. Each of the beamformer approaches requires, at a minimum, 180 times the computation effort, given a 2 degree resolution.

3. EXPERIMENTAL RESULTS

A multi-day PBD demonstration was conducted off of North Western Europe in February 2015. The Very Low Frequency (VLF) PBD shown in Figure 5 was deployed in a Navy range at a depth of 160 meters. The operating bandwidth was 1300 Hz at a center frequency of 1440 Hz. The unit made DOA measurements every 4 seconds, and continuously recorded the basebanded data from all 4 hydrophones. It operated continuously for nearly 4 days.

Targets included various ships of opportunity, including the deployment ship, and specifically a target simulator transmitting a continuous, time-varying broadband signal within our operating band. The target simulator was programmed to make looping runs past the PBD at various ranges. The environmental conditions varied dramatically over the four days.

Figure 1 shows the PBD DOA estimates for a portion of one day. In the following, we make arbitrary extractions from the entire data set to exercise our Matlab-based tracker. In the following plots of Figure 6, we show the PBD estimates as faint "x" marks, with the output of our tracker superimposed in three colors. The green trace shows the initiation of a track, the black shows an established track, and the red line shows the projection of an already established track which cannot make a proper association with the newest PBD estimate.

Fig. 5. The VLF PBD

The second level plots show close-up details of the 4 longest tracks developed from the extracted data set. Note that, while the upper plot shows time in hours, the lower plots show time in seconds. This shows the time that the specific "target" was held as a single track. Although in many cases the human eye can find association among nearby tracks, our tracker presently is unable to do so.

We note that the tracker presently employed does not account for the 0 – 360 degree discontinuity from the compass. Later versions will address this problem.

We are able to associate the specific time along a track at which to extract and analyse single-hydrophone time series. Figure 6 shows a large black arrow, which indicate the time that we extracted and analysed time series. We provide time-frequency analyses of the data using a 50% overlapped spectrogram, with the results displayed in decibels. Figure 7 shows two plots, the left hand side showing the spectrogram using an 8-bit gray scale, the second plot showing results with a 4-bit gray scale. The differences will be discussed in the next section.

The regions in Figure 6 similar to that indicated by the arrow reflect times that the target simulator was making its looping runs about the range. It is likely, though uncertain, that all of the tracks for this 8+ hour run were made by the simulator. Note that each of the identified tracks exceed 30 minutes in duration, with track 1 exceeding 60 minutes.

The PBD properly tracked one ship of opportunity on one extremely unfavourable day, with high winds and noise, to a range of 3.5 km. It regularly tracked our support vessel to a range in excess of 5 km.

4. TIME SERIES ANALYSES

In those cases in which the PBD is configured to extract and/or record received time series, we have developed (in Matlab) the ability to perform time-frequency analyses on selected snippets of noise. For the time indicated by the arrow in Figure 6, we extracted 1 minute of baseband data from one hydrophone, to produce the spectrograms of Figure 7. These spectrograms are consistent with the known radiated signature of the target simulator. We note that the number of bits used to represent the 8-bit (256 level) spectrogram is 40.2 million, while the 4-bit spectrogram requires 2.5 million bits

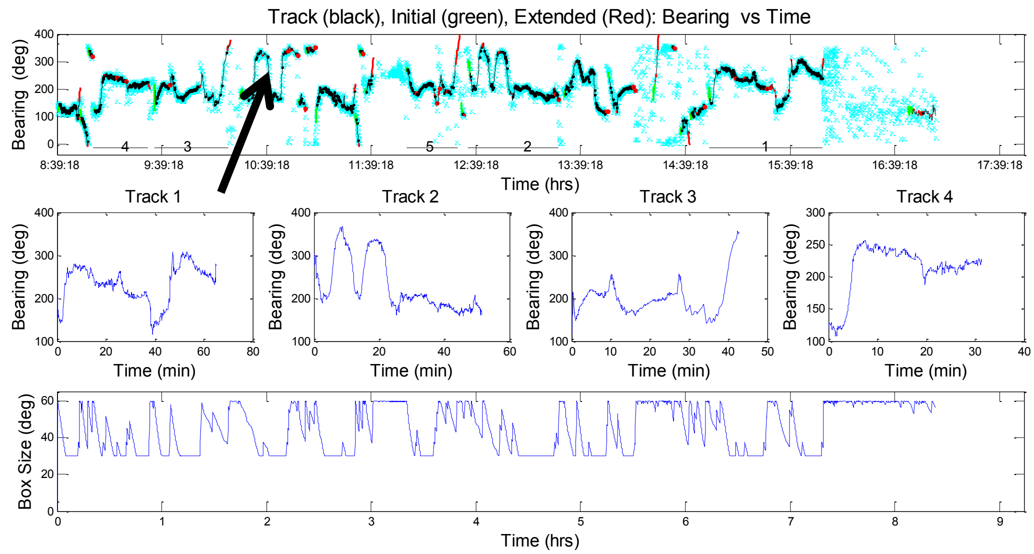

Fig. 6. PBD bearings (cyan "x") with superimposed tracks (green, black and red) in the upper plot. Horizontal lines beneath the tracks are numbered and show the 5 longest tracks. The top 4 tracks are shown in the 4 middle plots. The lower plot shows the tracker observations window as it opens and closes, depending on the track quality. The black arrow indicates a region for time series analyses.

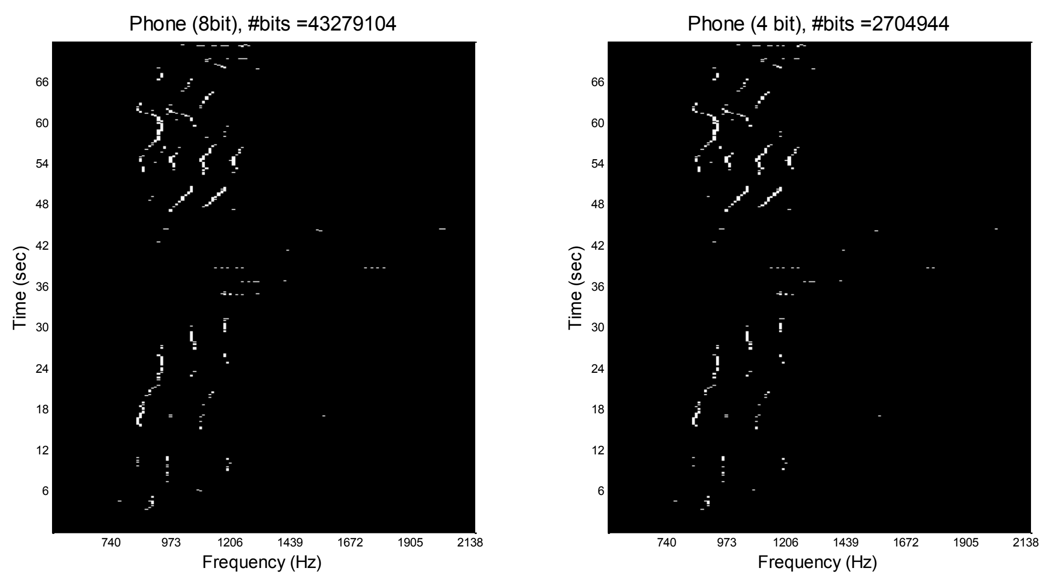

Fig. 7. 8-bit and 4-bit spectrograms for 1 minute of time series extracted about the time indicated by the black arrow in Figure 6.

The 4-bit spectrogram is perhaps sufficient for most applications, but experience is required to verify this observation. In terms of transmittal of the spectrogram to a remote observer via acoustic communications, the number of bits required even for the 4-bit spectrogram is excessive. We have implemented a version of lossless run-length coding to compress both spectrograms, as shown in Figure 8. These plots show perfect reconstruction when compared to Figure 7, but require only 22.2 Kbits and 18.4 Kbits, respectively, either of which is feasible with acoustic communications. We also note that track-specific spectrograms do not necessarily need to be of such long duration.

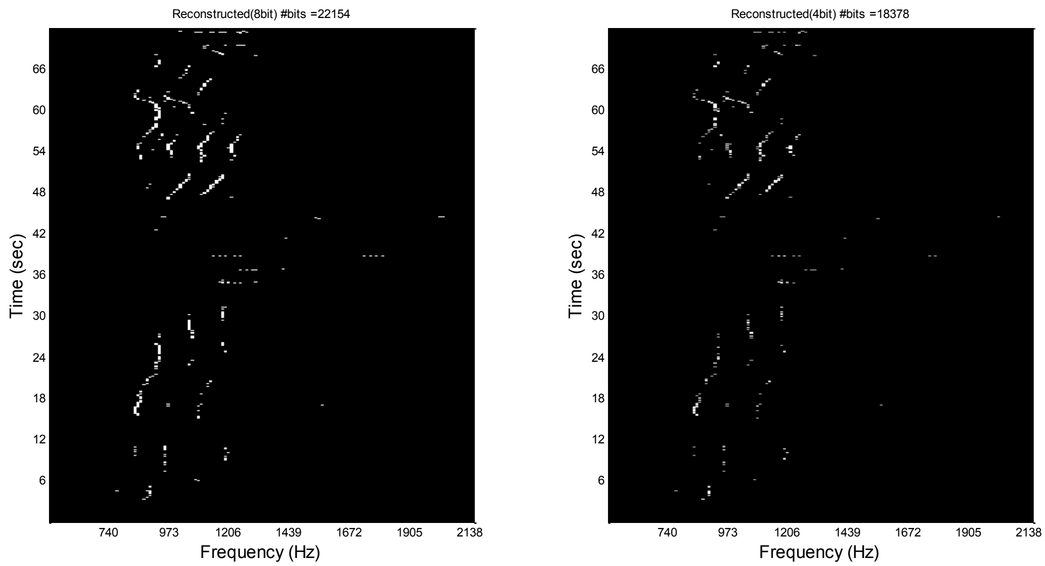

Fig. 8. Run-length encoded and reconstructed 8-bit and 4-bit spectrograms pertinent to those of Figure 7.

5. CONCLUSIONS

The PBD is an extension of Teledyne Benthos' core acoustic communications technology and is built upon our modem-based positioning systems. The device will provide accurate DOAs for any broadband energy source with sufficient energy contained within the operating bandwidth. Typical PBD systems have been built to operate between 900 – 1900 Hz, 9 – 14 kHz, and 22 – 27 kHz, with the only significant difference being the aperture of the tetrahedral array. Successful tests and demonstrations have been conducted in Massachusetts, Florida, and Hawaii in the USA, and in Northern Europe.

The PBD is best used in restricted areas, or otherwise where little shipping is anticipated. Being an interferometric device it is designed to respond to one source of energy only, and may experience biases and other errors when competing energy sources are present. An ideal application is for observing intrusion into marine preserves, such as the Papahānaumokuākea Marine National Monument in the Northern Pacific Ocean, shown in Figure 9. However, as shown here, provided the "desired" source is sufficiently stronger (about 3 dB) than competing sources, the PBD will faithfully lock on to that source.

A low frequency PBD has the ability to continuously record all 4 channels of time series as well as to record and transmit (via the associated acoustic modem) measured and time-stamped DOA estimates. We have developed a Matlab-based tracker which does an excellent job of identifying and following what, to the human eye, appears to represent a track from a discrete energy source. We have extended the tracker to extract up to one minute of time series from one hydrophone and to conduct time-frequency analyses of the data, followed by significant compression to prepare the spectrogram for transfer via acoustic modem.

Fig. 9. The Papahānaumokuākea Marine National Monument

The tracker and its extensions will soon be implemented into the real-time DSP environment.

6. REFERENCES

[1] D. Green, S. McManus, ”A New Technology For Broadband Passive Bearing Estimation,” Oceans 2014 Canada

[2] W. Liu, S. Weiss, *Wideband Beamforming, Concepts and Techniques*, Chichester, UK, Wiley, 2010.

[3]Yingbo Hua, et. al., Eds, “Conventional Subspace Methods,” in *High-Resolution and Robust Signal Processing*, CRC Press 2003, pp. 87-88